Acyl Chain Length and Saturation Modulate Interleaflet Coupling in Asymmetric Bilayers: Effects on Dynamics and Structural Order

Salvatore Chiantia* and Erwin London*
Department of Biochemistry and Cell Biology, State University of New York, Stony Brook, New York

ABSTRACT A long-standing question about membrane structure and function is the degree to which the physical properties of the inner and outer leaflets of a bilayer are coupled to one another. Using our recently developed methods to prepare asymmetric vesicles, coupling was investigated for vesicles containing phosphatidylcholine (PC) in the inner leaflet and sphingomyelin (SM) in the outer leaflet. The coupling of both lateral diffusion and membrane order was monitored as a function of PC and SM acyl chain structure. The presence in the outer leaflet of brain SM, which decreased outer-leaflet lateral diffusion, had little effect upon lateral diffusion in inner leaflets composed of dioleoyl PC (i.e., diffusion was only weakly coupled in the two leaflets) but did greatly reduce lateral diffusion in inner leaflets composed of PC with one saturated and one oleoyl acyl chain (i.e., diffusion was strongly coupled in these cases). In addition, reduced outer-leaflet diffusion upon introduction of outer-leaflet milk SM or a synthetic C24:0 SM, both of which have long interdigitating acyl chains, also greatly reduce diffusion of inner leaflets composed of dioleoyl PC, indicative of strong coupling. Strikingly, several assays showed that the ordering of the outer leaflet induced by the presence of SM was not reflected in increased lipid order in the inner leaflet, i.e., there was no detectable coupling between inner and outer leaflet membrane order. We propose a model for how lateral diffusion can be coupled in opposite leaflets and discuss how this might impact membrane function.

INTRODUCTION

Signal transduction in the plasma membrane (PM) requires the passage of information from outside a cell to inside and is usually triggered by clustering or activation of receptors in the outer leaflet, i.e., on the extracellular side (1). The organization of membrane lipids may influence this process. According to the raft model for PM organization, protein-protein interactions are governed by the formation of ordered protein-lipid domains enriched in cholesterol and sphingolipids, such as sphingomyelin (SM) (2). Due to the compositional asymmetry of the PM, SM is mostly found in the outer leaflet, whereas unsaturated phospholipids with ethanolamine-, serine-, or inositol-based headgroups are largely or fully localized in the inner leaflet (3,4). As a consequence, only the outer-leaflet lipid composition can support raftlike domain formation, whereas inner-leaflet lipid mixtures produce membranes that are homogeneous and cannot form rafts by themselves (5). Nevertheless, membrane domain formation in the outer leaflet somehow influences the lateral organization of inner-leaflet-associated proteins during signal transduction (1,6). This raises the question of whether and how the inner and outer leaflets influence each other's properties (i.e., the question of interleaflet coupling). Identifying the molecular determinants of interleaflet coupling might be instrumental in designing methods to influence the multitude of biological processes that rely on signaling through the PM.

Several biophysical studies have addressed this interesting issue, focusing especially on the formation of lipid domains in the inner leaflet in response to lipid-domain formation in the outer leaflet of a model bilayer (7–11). It is clear that lipids play an important role in interleaflet interaction and that proteins spanning the whole bilayer are not strictly required.

Specific molecular mechanisms determining interleaflet coupling have been suggested in the past, and examples include cholesterol transbilayer dynamics, electrostatic interaction, and lipid acyl chain interdigitation (12,13). The latter, in particular, was the subject of early investigations (14) showing how asymmetric sphingomyelin (i.e., SM with an amide-linked acyl chain much longer than the sphingoid base) could make the inner leaflet respond to the physical state of the outer leaflet. To date, it is not clear whether acyl chain interdigitation might be important in lipid mixtures of biological relevance (12). However, it is worth noting that experimental studies investigating interdigitation as a mechanism of leaflet-leaflet interaction have been performed so far only on symmetric membranes (14,15) or on phospholipid monolayers supported on immobile hydrocarbon films (16) and that the importance of the compositional asymmetry of PM lipids might therefore have been underestimated in those studies. To date, consensus about the molecular prerequisite for the interaction between leaflets has not been reached.

In this study, we use free-standing model membrane vesicles with an asymmetric lipid distribution to determine the minimum requirements for interleaflet coupling. By changing the structure of lipid acyl chains (i.e., length and saturation), we show that acyl chain interdigitation can

Submitted September 24, 2012, and accepted for publication October 26, 2012.

*Correspondence: erwin.london@stonybrook.edu or chiantia@gmail.com

Editor: Claudia Steinem.

0006-3495/12/12/2311/9 $2.00
http://dx.doi.org/10.1016/j.bpj.2012.10.033

decrease the lateral diffusion of inner-leaflet lipids in the presence of an ordered outer leaflet, i.e., induce coupling of diffusion. Interestingly, we also find that the coupling between dynamics of the inner and the more ordered outer leaflet is not necessarily connected to coupling of structural order between the two leaflets.

MATERIALS AND METHODS

All material and methods used in this work are described in the Supporting Material.

RESULTS

Sphingomyelin with a very long acyl chain increases interleaflet coupling

To determine the effect of acyl chain length and interdigitation on interleaflet coupling, we prepared asymmetric giant unilamellar vesicles (GUVs) with an inner leaflet composed of dioleoylphosphatidylcholine (DOPC) and an outer leaflet composed of DOPC and SM from different natural sources, i.e., porcine brain (bSM) or bovine milk (mSM). Whereas the most abundant molecule in bSM mixtures is C18:0 SM, mSM is enriched in SM with acyl chains that are significantly longer than the sphingoid base (i.e., C22:0 SM, C23:0 SM, and C24:0 SM) and can reach into the opposing monolayer (17). We probed the physical properties of each leaflet in several asymmetric GUVs by measuring the diffusion of labeled lipids via fluorescence correlation spectroscopy (FCS). As an improvement over our previous approach (18), the fluorescent probe pair NBD-DOPE/Atto-SM was used. This allowed us to investigate both leaflets of a single GUV within one single experiment. Relative to using a single probe in each vesicle preparation, this reduces both the number of samples needed and the large statistical uncertainty due to the asymmetric GUV compositional heterogeneity.

Fig. 1 *A* shows the relative lateral diffusion coefficient (D) of NBD-DOPE in the inner leaflet (D_{inner}) of several vesicles as a function of the relative D of Atto-SM in the outer leaflet (D_{outer}) of the same vesicles. All the D values reported are scaled to that measured for a symmetric DOPC GUV (i.e., D ~ 10 $\mu m^2/s$ (18,19)), both for the outer (*x* axis) or the inner leaflet (*y* axis) as described in the Methods section. Representative FCS autocorrelation curves are shown in Fig. S1 in the Supporting Material. Due to the ordering effect of SM, the outer leaflet has relatively slower dynamics, as shown by the fact that all the asymmetric GUVs exhibit a D in the outer leaflet of 40–80% of D in the outer leaflet of a symmetric DOPC GUV (i.e., D_{outer} is between 4 and 8 $\mu m^2/s$). The GUV-to-GUV variation is due also to the fact that we varied the amount of SM exchange in different vesicles by varying MβCD (and at the same time SM) concentration during lipid exchange. When comparing

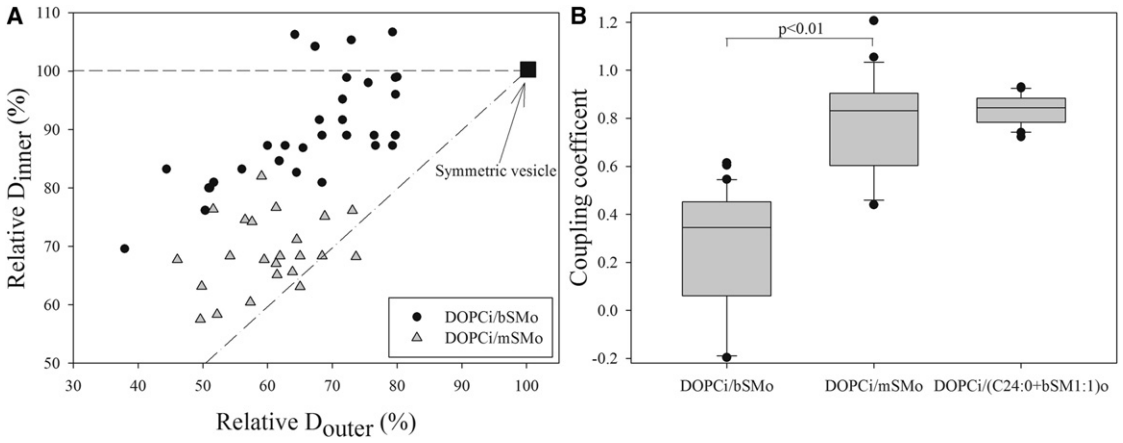

FIGURE 1 Interleaflet coupling is influenced by SM acyl chain length. (*A*) Diffusion coefficient of NBD-DOPE in the inner leaflet as a function of the diffusion coefficient of Atto-SM in the outer leaflet. *D* values are shown as a percentage of the value measured for the same leaflet localization of the probes in a symmetric DOPC vesicle. Each black circle refers to a single DOPCi/bSMo GUV. Gray triangles refer to single DOPCi/mSMo vesicles. Notice that in all cases shown here, and in later figures, after exchange the outer leaflet contains a mixture of SM and residual inner leaflet PC. The square in position (100, 100) indicates the relative *D* values measured in a symmetric DOPC GUV. The dash-dotted line has unitary slope (i.e., maximum coupling); the dashed line has null slope (i.e., zero coupling). (*B*) Box plot of the coupling coefficients measured for each asymmetric GUV in three different types of sample. The median, the lower quartile, and the upper quartile are shown as a line inside, and the lower and upper horizontal boundaries, respectively, of the solid rectangles. The ends of the whiskers represent the 9th and 91st percentiles of the observed data. Two lower outliers for the DOPCi/bSMo sample were removed for presentation. The coupling coefficients are calculated as the slope of the lines connecting each point in *A* with the (calibration) symmetric GUV in position (100, 100). The coupling coefficients calculated for DOPCi/mSMo vesicles are significantly different from those calculated for the DOPCi/bSMo vesicle, with $p < 0.01$ measured by Student's *t*-test. The numbers of analyzed vesicles were 32 from four independent preparations with bSMo; 24 from three independent preparations with mSMo; 20 from two independent preparations with a 1:1 (mol:mol) mixture of C24:0SM and bSM introduced into the outer leaflet, i.e. (C24:0 + bSM 1:1)o. Independent preparations were produced using different SM/MβCD concentrations, ranging from 42.5 to 57 mM MβCD, in the donor solution. Vesicles with a relative diffusion in the outer leaflet >80% (i.e., 8 $\mu m^2/s$) were excluded from further analysis and are not represented in the figure.

GUVs with similar relative D_{outer}, it appears clear that the diffusion in the inner leaflet of DOPCi/bSMo GUVs (*black circles*) (see Materials and Methods in the Supporting Material for sample nomenclature) is in general faster than that measured for DOPCi/mSMo GUVs (*gray triangles*). This means that diffusion in the inner and outer leaflets is more similar if mSM, rather than bSM, is present in the outer leaflet. To quantify the similarity/coupling between the leaflets, we compared each GUV with the symmetric control and calculated the ratio $(10\,\mu m^2/s - D_{inner})/(10\,\mu m^2/s - D_{outer})$, assuming D ~ 10 $\mu m^2/s$ for both leaflets before the introduction of SM. These ratios are referred to as coupling coefficients, and they can be visualized as the slope of the lines connecting the (100%, 100%) control symmetric GUV point to each asymmetric GUV data point. Coupling coefficients calculated from several GUVs with different compositions are shown in Fig. 1 *B*. Vesicles with a low degree of outer-leaflet exchange (D_{outer} > 80%, i.e., >8 $\mu m^2/s$) were not evaluated, because their proximity to the (100%, 100%) point would introduce a large variation in slope calculations.

This analysis reveals that diffusion in the inner leaflet of DOPCi/bSMo is only weakly influenced by decreased diffusion in the outer leaflet after the introduction of bSM (average coupling coefficient, 0.26), in agreement with our previous measurements (18). In contrast, in DOPCi/mSMo GUVs, the inner leaflet is strongly coupled to the outer leaflet (average coupling coefficient, 0.78). Similar results were observed using NR12S to label separately the inner and the outer leaflets of DOPCi/mSMo GUVs (data not shown). To verify whether the increased coupling in DOPCi/mSMo samples was indeed due to the presence of long acyl chains in mSM molecules, we prepared asymmetric GUVs with DOPC in the inner leaflet and a mixture of bSM and synthetic C24:0 SM (1:1 molar ratio) in the outer leaflet. These DOPCi/(C24:0 + bSM)o GUVs were characterized by coupling coefficients comparable to those measured in DOPCi/mSMo GUVs (average coupling coefficient, 0.84), the only difference in this case being a considerable decrease in sample heterogeneity (as shown by the smaller spread of the points in Fig. 1 *B* for this mixture).

PCs with one saturated acyl chain increase interleaflet coupling

We next analyzed the effect of PC acyl chain structure upon interleaflet coupling. We first prepared POPCi/bSMo GUVs and compared them to the DOPCi/bSMo GUVs as described in the previous paragraph. Fig. 2 *A* shows the relative D_{inner} and D_{outer} for these two compositions of asymmetric GUVs. After introduction of bSM into the outer leaflet, the presence of POPC in the inner leaflet of the GUVs seems to be associated with slower dynamics in the inner leaflet relative to that of DOPCi/bSMo GUVs. (Note that for the calculation of relative diffusion coefficients, diffusion of POPCi/bSMo GUVs was scaled to that measured in symmetric POPC GUVs, analogous to the scaling of DOPCi/bSMo diffusion to that of DOPC GUVs.) Similar results were observed using NR12S to label separately the inner and the outer leaflets of POPCi/bSMo GUVs (data not shown). We then performed analogous experiments using other PCs consisting of one saturated and one oleoyl chain as

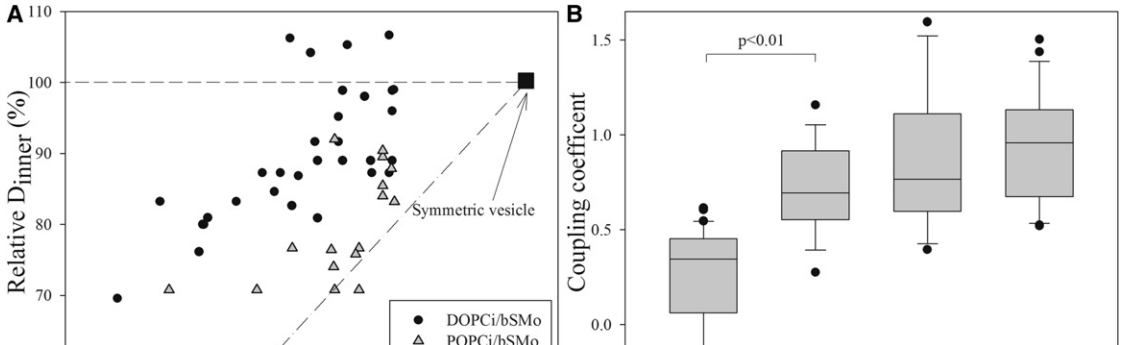

FIGURE 2 Interleaflet coupling is influenced by PC acyl chain saturation. (*A*) Diffusion coefficient of NBD-DOPE in the inner leaflet as a function of the diffusion coefficient of Atto-SM in the outer leaflet, relative to the value measured with the same configuration of the probes but in a symmetric DOPC or POPC vesicle. Each black circle refers to a single DOPCi/bSMo GUV. Gray triangles refer to POPCi/bSMo vesicles. The point in position (100, 100) indicates the normalized *D* values measured in a symmetric DOPC or POPC GUV. The dash-dotted line has unitary slope (i.e., maximum expected coupling); the dashed line has null slope (i.e., zero coupling). (*B*) Box plot of the coupling coefficients measured for each asymmetric GUV with bSM in the outer leaflet and different PCs in the inner leaflet. The coupling coefficients calculated for DOPCi/bSMo vesicles are, as an ensemble, significantly different from those calculated for the POPCi/bSMo vesicle, as measured by Student's *t*-test, $p < 0.01$. The numbers of analyzed vesicles were 32 from four independent preparations with DOPCi; 16 from two independent preparations with POPCi, 22 from two independent preparations with SOPCi; and 22 from two independent preparations with OMPCi. Independent preparations were produced using different MβCD concentrations, ranging from 50 to 57 mM, in the donor solution. Vesicles with a relative diffusion in the outer leaflet >80% were excluded from further analysis and are not represented in the figure.

inner-leaflet lipids, i.e., stearoyl-oleoyl PC (SOPC) and 1-oleoyl-2-myristoyl-*sn*-glycero-3-phosphocholine (OMPC). Fig. 2 *B* shows a quantitative comparison of all the asymmetric GUV samples containing bSM in the outer leaflet and different PCs in the inner leaflet. The average inter-leaflet coupling coefficient for POPCi/bSMo (0.73) was indeed significantly higher than those measured for DOPCi/bSMo vesicles (0.26). A high average coupling coefficient was also observed for SOPCi/bSMo (0.85) and OMPCi/bSMo (0.94).

Inner-leaflet structural order is not increased in POPCi/bSMo asymmetric membranes

As described in the previous paragraph, we consistently observed slower lipid dynamics in asymmetric GUVs with one saturated and one unsaturated acyl chain in the inner leaflet compared to DOPCi/bSM GUVs. Therefore, attention was focused on comparing POPCi/bSMo vesicles to DOPCi/bSMo for studies of membrane order. To probe the physical state of the inner leaflet, we performed fluorescence lifetime imaging (FLIM) of asymmetric GUVs containing 1,2-dipalmitoyl-*sn*-glycero-3-phosphoethanolamine-*N*-(7-nitro-2-1,3-benzoxadiazol-4-yl) (NBD-DPPE) in the inner leaflet. The fluorescence lifetime of NBD lipids is sensitive to bilayer order (20,21). The advantage of using this molecule is that NBD in the outer leaflet can be selectively destroyed with dithionite to obtain a signal arising exclusively from the inner leaflet (22). When included in lipid vesicles, NBD-DPPE has a two-component fluorescence lifetime decay. The fluorescence lifetimes for both components (i.e., $\tau1 \sim 2$–3 ns and $\tau2 \sim 8$–9 ns) increase as the amount of bSM (and thus membrane order) increases, although the relative amplitudes of each component ($\tau1/\tau2 \sim 2{:}1$) are nearly constant in all lipid compositions studied (data not shown). We found that the dependence of $\tau1$ on bSM molar concentration is larger and more reproducible compared to that of $\tau2$ (Fig. S2), so $\tau1$ was used to evaluate membrane order. Several FLIM images were acquired for each sample and analyzed by calculating lifetime histograms for the pixels in the zones of interest and fitting them with the appropriate mathematical model (Fig. S3).

Fig. 3 *A* shows $\tau1$ values in symmetric DOPC, POPC, and the corresponding asymmetric PCi/bSMo GUVs. For the asymmetric GUVs, both the average $\tau1$ from the inner- and outer-leaflet NBD-DPPE before outer-leaflet reduction (*gray bars*) and the inner-leaflet $\tau1$ after reduction of outer-leaflet NBD (*black bars*) are shown. It should be noted that a two-component model does not accurately fit the data for GUVs labeled in both leaflets (probably because they result from the superposition of different inner- and outer-leaflet values), and therefore, only an approximate value for $\tau1$ can be provided in this case. Nevertheless, it is clear that overall $\tau1$ increases after the introduction of SM into the outer leaflet to form asymmetric GUVs (note that inner- and outer-leaflet $\tau1$ values are nearly identical in symmetric DOPC and POPC vesicles; see Fig. S2). In contrast, the inner leaflet exhibits only a very small change for both DOPCi/bSMo and POPCi/bSMo GUV, suggesting that the inner leaflet remains fully disordered after SM introduction. This is indicative of at most only a low extent of coupling between inner- and outer-leaflet order, in agreement with previous studies (23,24).

To obtain more precise information about coupling between inner- and outer-leaflet order, the studies were extended to asymmetric small unilamellar vesicles (SUVs), which have several advantages: 1), they can be studied with a larger variety of spectroscopic methods compared to GUVs; 2), there are more methods to more readily individually label inner or outer leaflets; and 3), asymmetric SUVs can be prepared with a very high degree of SM substitution (>80%) in the outer leaflet (24). First, membrane

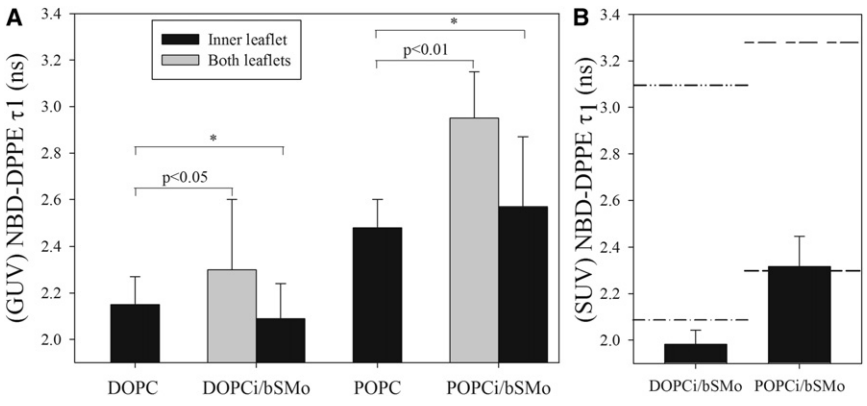

FIGURE 3 Probing the state of the inner leaflet using the fluorescence lifetime of NBD-DPPE in asymmetric GUVs and SUVs. (*A*) Fast fluorescence lifetime component of NBD-DPPE ($\tau1$) in symmetric and asymmetric GUVs as calculated from FLIM. At least six images from two independent preparations were analyzed for each lipid composition (see Fig. S3). $\tau1$ measured for the inner leaflet of symmetric DOPC GUVs is significantly different from $\tau1$ measured for both leaflets of asymmetric DOPCi/bSMo GUVs (*t*-test $p < 0.05$). $\tau1$ measured for the inner leaflet of symmetric POPC GUVs is significantly different from $\tau1$ measured for both leaflets of asymmetric POPCi/bSMo GUVs (*t*-test $p < 0.01$). The asterisk indicates data sets statistically not distinguishable by *t*-test. Error bars represent standard deviations. (*B*) Short fluorescence lifetime component of NBD-DPPE $\tau1$ in asymmetric SUVs of varying composition. Lines are reference values for symmetric DOPC inner leaflet (*dash-dotted line*), symmetric POPC inner leaflet (*dashed line*), symmetric DOPC/bSM 1:4 inner leaflet (*dash-dot-dotted line*) and symmetric POPC/bSM 1:4 inner leaflet (*short-dash-long-dashed line*). All the reported values were obtained from four measurements in two independent preparations. Error bars represent the standard deviations.

order was evaluated by fluorescence lifetime measurements in asymmetric DOPCi/bSMo and POPCi/bSMo SUVs with NBD-DPPE, analogous to the experiments on GUVs. As shown in Fig. 3 *B* and Fig. S2, membrane order measured through $\tau 1$ is much higher in symmetric DOPC/bSM 1:4 or POPC/bSM 1:4 SUVs than in DOPC or POPC vesicles, respectively. However, inner-leaflet $\tau 1$ did not increase upon introduction of SM in the outer leaflet for either DOPCi/bSMo or POPCi/bSMo SUVs, confirming the results obtained for GUVs.

To further confirm these results, two other methods for defining membrane order were employed. The first approach made use of the solvatochromic properties of NR12S. This molecule is sensitive to the hydration of the lipid monolayer (and therefore to the lipid packing). To restrict the NR12S signal to the inner leaflet, it was quenched in the outer leaflet by reduction with sodium dithionite (25). Using this approach, we measured the emission spectrum of NR12S confined in the inner leaflet of asymmetric SUVs that had bSM in the outer leaflet and either DOPC or POPC in the inner leaflet. As shown in Fig. 4 *A*, for both asymmetric membrane compositions, the NR12S emission spectrum had a peak at ~599 nm. This value is very similar to that measured when NR12S is in the inner leaflet of symmetric DOPC or POPC bilayers, and it is much higher than that measured in the inner leaflet of vesicles with a 1:4 PC/bSM composition. In contrast, NR12S emission shows that for both POPCi/bSMo and DOPCi/bSMo SUVs, the outer leaflet was considerably more ordered than that of pure fluid PC bilayers (Fig. S4). These data, which are consistent with the NBD-DPPE lifetime data, show that the hydration/packing of the inner leaflet of these asymmetric SUVs is not influenced by the presence of a more ordered outer leaflet.

Finally, as a direct measure of membrane order, the steady-state fluorescence anisotropy of the probe 4′-(trimethylammonio)diphenylhexatriene p-toluenesulfonate (TMA-DPH) was evaluated (26). For these experiments, we used our recently developed methods of preparing vesicles with TMA-DPH only in the inner or only in the outer leaflet of SUVs (27). As shown in Fig. 4 *B*, the outer leaflet of asymmetric vesicles is highly ordered due to the presence of bSM. In the cases of both DOPCi/bSMo and POPCi/bSMo SUVs, the anisotropy of TMA-DPH in the outer leaflet is ~0.31, comparable to the values observed for symmetric DOPC (or POPC) vesicles with 80 mol % bSM (i.e., ~0.30), as expected. On the other hand, the inner leaflet for both of the above-mentioned compositions is much more disordered, with anisotropy values only slightly higher than those measured in symmetric DOPC or POPC vesicles (i.e., ~0.23). In DOPCi/mSMo (Fig. 4 *B*), SOPCi/bSMo, and OMPCi/bSMo SUVs (data not shown for the latter two compositions), we observed the same pattern of low order in the inner leaflet and, thus, weak coupling to the high degree of order in the outer leaflet. All three methods used demonstrated that there was no coupling or weak coupling of order in all the cases in which there was strong coupling of inner- and outer-leaflet dynamics.

In summary, these data show that 1), all the acyl chain compositions we have tested produce asymmetric lipid bilayers with an inner leaflet much less ordered than the outer one, and 2), for all the acyl chain compositions studied, the structural order in the inner leaflet is at most weakly influenced by the outer leaflet.

DISCUSSION

Acyl chain interaction at bilayer midplane couples lipid dynamics in the two opposing leaflets

We have investigated the physical interaction between the two leaflets of asymmetric free-standing membranes using asymmetric GUVs and SUVs with simple lipid compositions. These advanced artificial membrane systems provide

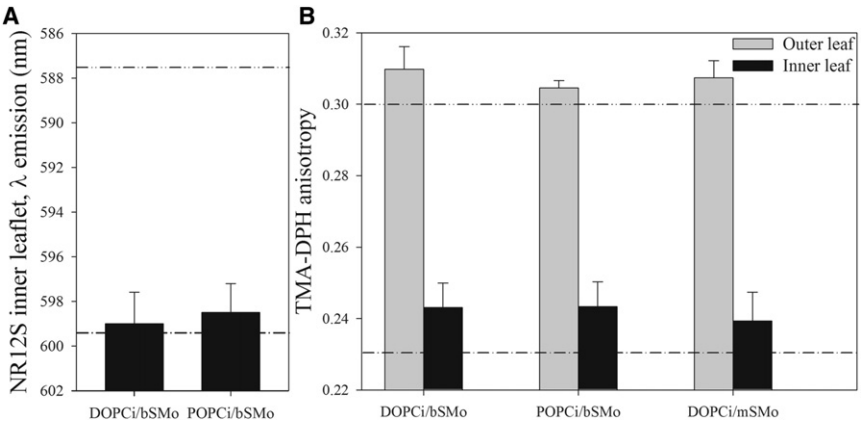

FIGURE 4 Interleaflet coupling is not detected by either TMA-DPH anisotropy or NR12S emission wavelength. (*A*) Maximum emission wavelength of NR12S in the inner leaflet of asymmetric SUVs with varying composition. Lines are reference values for symmetric DOPC inner leaflet (*dash-dotted line*), and symmetric DOPC/bSM 1:4 inner leaflet (*dash-dot-dotted line*). Reference values for symmetric POPC and symmetric POPC/bSM 1:4 are within ±1 nm of those indicated for symmetric DOPC and symmetric DOPC/bSM 1:4, respectively. All the reported values were obtained from four measurements in two independent preparations, and the error bars represent standard deviations. (*B*) TMA-DPH anisotropy measured either in the outer (*gray*) or inner leaflet (*black*) of asymmetric SUVs with varying composition. Lines are reference values for symmetric DOPC (*dash-dotted line*) and symmetric DOPC/bSM 1:4 (*dash-dot-dotted line*). Reference values for symmetric POPC and symmetric POPC/bSM 1:4 are within ±0.01 of those indicated for symmetric DOPC and symmetric DOPC/bSM 1:4, respectively. All the reported values were obtained from four measurements in two independent preparations, and the error bars represent standard deviations.

a more effective model than those previously developed for studying the structure of cellular plasma membrane, and they have allowed, for the first time, to our knowledge, a detailed investigation of the effect of acyl chain interdigitation upon interleaflet coupling.

Previous experimental studies on symmetric model systems have suggested that interleaflet interaction might be significant in the presence of asymmetric lipids with acyl chains that can interdigitate into the opposing leaflet (14). Recent studies on more advanced PM models (i.e., asymmetric supported bilayers with biologically relevant compositions) reported that domain formation in the inner leaflet and interleaflet coupling might also depend on the melting temperature (Tm) of its lipid components (8). In other words, if the outer leaflet forms ordered-state domains, inner-leaflet lipids with high ordered/disordered Tm ratios would most readily couple with the outer-leaflet lipids. Based on these premises, we have prepared asymmetric vesicles with simple but specifically tailored compositions. The outer leaflet contained either a weakly interdigitating or highly interdigitating SM. This choice was dictated by the fact that asymmetric sphingolipids have been shown to be directly involved in raft function and signaling through the PM (28–30). For the inner leaflet, we selected four PCs with different acyl chains and L_β/L_α Tm (-18 to $+7$°C (31)): DOPC, OMPC, POPC, and SOPC. Of these, the latter two have the highest Tm values.

Our first observation was that acyl chain interdigitation due to the presence of very-long-chain SM increases physical interaction between the leaflets of asymmetric membranes (based on lipid diffusion data), as shown schematically in Fig. 5, *A* and *B*. In the presence of an SM-containing ordered outer leaflet, such an interaction hinders the diffusion of membrane components in the inner leaflet. This result is of interest in a biological context because it provides a physical model for the role of asymmetric sphingolipids in cellular processes, such as the modulation of signaling in neutrophils. Previous studies have shown that the clustering of lactosyl-ceramide (LacCer) triggers the clustering and activation of the Src kinase Lyn only if LacCer possesses very long acyl chains (28). We speculate that it is possible that the long interdigitating acyl chains are needed because they physically interact with the inner leaflet, thus affecting the dynamics and organization of its components, such as lipid-anchored kinases.

A second observation was that the interleaflet coupling observed via lipid lateral diffusion measurements does not necessarily require outer-leaflet lipids with very long and asymmetric acyl chains, but rather is detected in the presence of a number of lipids with just one saturated acyl chain, such as POPC. Interestingly, observations from the experiments in which we varied the inner-leaflet composition suggest that stronger interleaflet coupling is not simply correlated with a higher melting temperature of the inner-leaflet lipids. In particular, substituting DOPC with OMPC

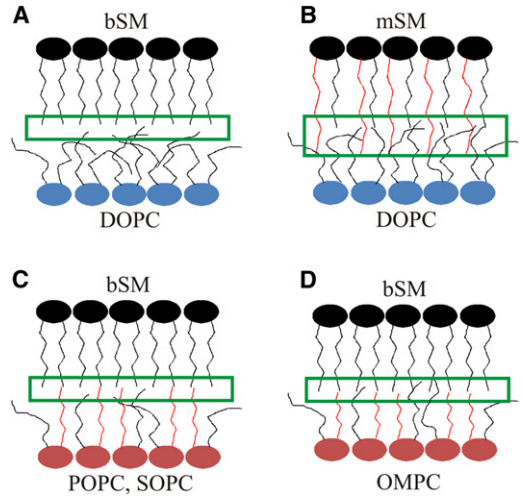

FIGURE 5 A model for how acyl chain composition influences interleaflet coupling. Schematic models of asymmetric bilayers with inner leaflets composed of DOPC (*blue*) (*A* and *B*) or a partially saturated PC, i.e., POPC, SOPC, or OMPC (*red*) (*C* and *D*). The outer leaflet is composed in all cases of SM (mSM (*B*) and bSM (*A*, *C*, and *D*)). The green rectangles indicate regions near the bilayer midplane, where acyl chains from an opposing leaflet might interact. Red lines represent the long interdigitating acyl chains of mSM in B, and the saturated PC acyl chains in *C* and *D*.

in the inner leaflet caused a significant increase in interleaflet coupling in terms of lipid diffusion, but data on PC melting temperatures versus acyl chain structure indicate that OMPC bilayers exhibit a melting temperature comparable to or even lower than that of DOPC bilayers (31,32). (The $L\beta/L\alpha$ Tm is -18°C for DOPC bilayers and -26°C for OMPC bilayers. The $Lc/L\alpha$ melting temperature is -12°C for DOPC and -8°C for OMPC.)

In general, an important factor to consider is the degree of physical proximity of lipid acyl chains belonging to the opposing leaflets at the bilayer midplane. It has been reported, for example, that the degree of structural disorder in DOPC bilayers can be so high that the oleoyl acyl chain may occasionally be bent back, bringing the CH_3 groups close to the water-membrane interface, which may reduce the carbon-atom density near the midplane (33). We argue that the saturated acyl chain of POPC stretches toward the bilayer center to a greater degree than does DOPC, increasing the probability of finding CH_3 groups in proximity to the bilayer midplane, where they can interact directly, via van der Waals interactions, with the acyl chains from the opposing leaflet. Such a transient interaction, e.g., with the acyl chain of a slowly diffusing SM molecule in the outer leaflet, might in turn result in increased interleaflet friction and thus hindered dynamics of diffusing lipids in the inner leaflet. This assumption is supported by both experimental and in silico data, suggesting a more stretched conformation of the oleoyl acyl chain (34) and a higher density of methyl groups at the bilayer midplane (i.e., a deeper electron density trough (35)) for POPC compared

to DOPC lipids. Furthermore, we calculated the average distance between the CH_3 groups in one leaflet and those in the opposing leaflet, using literature data from molecular-dynamics all-atom simulations of symmetric membranes with different compositions (Fig. S5). In line with the above considerations, this distance is significantly smaller in the case of bilayers composed of lipids with one saturated acyl chain (i.e., POPC or SOPC) compared to DOPC (schematically illustrated in Fig. 5, *A* and *C*). This pattern is well correlated with our data on interleaflet coupling from lipid lateral-diffusion measurements. Of course, the above considerations do not exclude the possibility of a role for PC acyl chain interdigitation in the asymmetric membranes examined. Given the difference in the depth of 1-position and 2-position acyl chains in PC molecules (36), this might be especially influential in the case of OMPC, which has a very short 2-position chain (Fig. 5 *D*). Our data suggest that enhanced interaction at the bilayer midplane between acyl chains from opposing leaflets does not require, in general, the extensive degree of acyl chain interdigitation expected in the case of mSM-containing membranes, because it is also observed in the presence of lipids with one saturated and one unsaturated chain that are comparable in length (e.g., SOPC). The common denominator between the cases in which we observe interleaflet coupling of lipid diffusion (i.e., strong interdigitation versus the presence of one saturated acyl chain) would thus be the increased contact of lipid acyl chains belonging to the opposing leaflets at or near the bilayer midplane. A more detailed molecular picture of the acyl chain interactions (and interdigitation) in asymmetric membranes with the above-mentioned lipid compositions might be obtained from molecular-dynamics simulations, but such studies would be outside the scope of this work.

Interleaflet coupling of lipid dynamics is not strictly connected to structural ordering of the inner leaflet

Surprisingly, our experiments show that the interleaflet coupling observed in terms of hindered inner-leaflet dynamics does not correlate with the increase observed in inner-leaflet structural order in both asymmetric GUVs and SUVs. It is worth noting that recent results from our laboratory indicate that interleaflet coupling in terms of bilayer order does not seem to depend on membrane curvature or vesicle size (23,24). The combined NBD fluorescence lifetime, TMA-DPH anisotropy, and NR12S fluorescence emission data indicate that the inner-leaflet lipid packing is not affected by the presence of an ordered outer leaflet. This suggests that the inner leaflet remains in a homogeneous disordered state in all the cases we studied. This is also supported by the observation that fluorescence microscopy did not show any evidence of the presence of microscopic domains with uneven lateral distribution of NBD-DOPE in the inner leaflet (data not shown). Furthermore, if there were submicroscopic inner-leaflet domains with lipid packing and structural order considerably higher than that observed in the rest of the monolayer, we would have expected the inner leaflet of the asymmetric vesicles to exhibit higher TMA-DPH anisotropy values, because this probe partitions significantly into ordered phases and thus reports on the average physical state of the whole monolayer in which it is embedded (37).

The lateral organization of the outer leaflet is not as simple to analyze as that of the inner leaflet. In the case of asymmetric SUVs, the high degree of exchange of SM (~80 mol %) and high anisotropy indicates that the outer leaflet is predominantly, and probably fully, in the highly ordered gel phase (23,24). However, based upon measured D_{outer} and previous calibration measurements (18), asymmetric GUVs contained only ~20–50 mol % SM in their outer leaflet. Thus, the outer leaflet of asymmetric GUVs might either be in a homogeneous liquid phase (but one that is somewhat ordered due to the presence of SM) or contain submicroscopic ($<$200 nm, not detectable by optical microscopy) SM-rich gel domains (38). The two scenarios are not mutually exclusive. In both cases, we would expect (and do indeed observe) a gradual SM-dependent decrease of D_{outer} as SM content increases (see Eq. 3 in the Supporting Material).

It is most likely that the reduction of lipid diffusion in the inner leaflet discussed in the previous paragraph derives from either 1), coupling between a homogeneous, partly ordered outer leaflet and a homogeneous inner leaflet (i.e., D_{inner} is constant over the monolayer) or 2), localized coupling between submicroscopic ordered domains in the outer leaflet and a single-phase inner leaflet (i.e., D_{inner} has submicroscopic variations over the inner monolayer so that we detect an average decrease in D_{inner} due to resolution restraints). In either case, our experiments indicate the presence of lipid-composition-dependent transient interactions between acyl chains occurring at the bilayer midplane. Such an interaction might couple an ordered outer leaflet (or just the portions of it that are ordered, as discussed above) with an otherwise disordered inner leaflet. Interestingly, this coupling appears to be significant enough to affect lipid diffusion, but apparently not enough to modify the bulk structural order of the inner monolayer.

Using some simplifications, the coupling coefficients may provide quantitative information about the diffusion of lipids in the inner leaflet. For the situation depicted in case 1 above, one model would be that a portion of the lipids in the inner leaflet diffuse exactly as they would in a symmetric vesicle, with relative $D_{inner} = 100\% = 10\mu m^2/s \equiv D_{inner}^{fluid}$ (i.e., unaffected by the presence of the ordered outer leaflet), whereas the rest of the lipids interact with lipids in the outer leaflets, diffusing comparably slowly (i.e., D_{inner}=D_{outer} for this subset of lipids). Since D_{outer} is,

at best, just a factor of ~2 lower than D_{inner}, FCS would roughly report a weighted average of the two diffusing behaviors (Fig. S6 *A*). In this approximation, the coupling coefficient would simply be equal to the average fraction of lipids diffusing with $D_{inner} = D_{outer}$ (Fig. S6 *B*). For example, the coupling coefficient of 0.85 measured for SOPCi/bSMo would be equivalent to a situation in which 85% of the SOPC in the inner leaflet diffuses as slowly as the lipids in the outer leaflet.

For the situation depicted in case 2 above, the interpretation of the coupling constant is slightly different: we assume that a fraction d of the lipids in the inner leaflet at any given time diffuses in correspondence with gel domains in the outer leaflet (which occupy a fraction d of the total surface of the outer leaflet, assuming the case of a spatially homogeneous distribution of lipids in the inner leaflet). This subset of lipids exhibits an lower average diffusion coefficient compared to D_{inner}^{fluid}, due to friction with lipids in the gel domains of the outer leaflet ($D_{inner}^{gel} = f \times D_{inner}^{fluid}$, with $f \leq 1$). The coupling coefficient depends in this case on both d and f (see Fig. S6 *C* for details). For example, if gel domains occupy 50% of the outer leaflet surface ($d = 0.5$) and lipids diffusing in correspondence of outer leaflet gel domains diffuse 30% more slowly than those in the rest of the inner leaflet (i.e., $f = 0.7$), the expected coupling coefficient would be 0.53 (see legend Fig. S6).

What is the biological significance of an interleaflet coupling mechanism that affects the movement of membrane components without changing the monolayer structural order per se? Our data suggest that if the outer leaflet of the plasma membrane contains small, ordered SM-enriched domains, the inner leaflet would be locally (i.e., just in spatial correspondence to the SM domains) affected via interleaflet coupling, and that the extent of this effect would depend on the exact lipid structure. As a consequence, the inner leaflet might contain zones characterized by slower diffusion, without necessarily invoking separation into ordered and disordered domains. Certain membrane components diffusing in the inner leaflet might exhibit hindered dynamics when passing through the above mentioned slow-diffusion patches. As shown by the work of Nicolau et al. (39), these conditions are sufficient to induce dynamic segregation of membrane proteins in the inner leaflet in response to the formation of an ordered domain in the outer leaflet. More precisely, in the presence of a membrane domain characterized by slower diffusion, membrane components can become transiently trapped within it, even without having specific affinity for the domain (e.g., because the domain structural order is not different from the rest of the monolayer). This transient trapping would provide time for interactions between proteins to develop or rearrange.

Of course, this mechanism for sorting of inner-leaflet components does not exclude the concurrence of other coupling mechanisms, such as that in which phase separation in the outer leaflet of the plasma membrane can induce analogous (i.e., ordered versus disordered) phase separation in the inner leaflet and, consequently, reorganization of inner-leaflet components based on an increased or decreased affinity toward specific lipid phases. In this regard, the role of additional specific lipids (for example, cholesterol) in determining the nature and extent of interleaflet coupling in asymmetric GUVs with macroscopic phase separation should be the subject of future studies.

In conclusion, we have presented here an improved method to study, for each individual leaflet of a membrane, lipid dynamics of compositionally asymmetric GUVs. It is important to note that we have observed significant interleaflet coupling of lipid diffusion, which depends on both the length and saturation of lipid acyl chains. The molecular mechanism is likely to involve van der Waals interactions between the terminal portions of the acyl chains of facing lipids occurring at and near the bilayer midplane. In line with this observation, we suggest that fine tuning of the lipid composition might be used to influence interleaflet coupling in biological membranes and, consequently, signal transduction through the PM. We have also shown that the SM-rich outer leaflet does not greatly affect the structural order of the inner leaflet for the lipid mixtures examined.

SUPPORTING MATERIAL

Six figures and a detailed Materials and Methods section are available at http://www.biophysj.org/biophysj/supplemental/S0006-3495(12)01186-1.

Prof. A. Herrmann (Humboldt Universität zu Berlin) and his group members are gratefully acknowledged for providing access to fluorescence lifetime instrumentation. Dr. A. Arbuzova is acknowledged for constructive discussions.

This work was supported by National Science Foundation grant DMR1104367. S.C. is a Howard Hughes Medical Institute fellow of the Life Sciences Research Foundation.

REFERENCES

1. Simons, K., and M. J. Gerl. 2010. Revitalizing membrane rafts: new tools and insights. *Nat. Rev. Mol. Cell Biol.* 11:688–699.
2. Brown, D. A., and E. London. 2000. Structure and function of sphingolipid- and cholesterol-rich membrane rafts. *J. Biol. Chem.* 275:17221–17224.
3. Devaux, P. F. 1991. Static and dynamic lipid asymmetry in cell membranes. *Biochemistry.* 30:1163–1173.
4. Bretscher, M. S. 1972. Asymmetrical lipid bilayer structure for biological membranes. *Nat. New Biol.* 236:11–12.
5. Wang, T. Y., and J. R. Silvius. 2001. Cholesterol does not induce segregation of liquid-ordered domains in bilayers modeling the inner leaflet of the plasma membrane. *Biophys. J.* 81:2762–2773.
6. Simons, K., and D. Toomre. 2000. Lipid rafts and signal transduction. *Nat. Rev. Mol. Cell Biol.* 1:31–39.
7. Kiessling, V., C. Wan, and L. K. Tamm. 2009. Domain coupling in asymmetric lipid bilayers. *Biochim. Biophys. Acta.* 1788:64–71.
8. Wan, C., V. Kiessling, and L. K. Tamm. 2008. Coupling of cholesterol-rich lipid phases in asymmetric bilayers. *Biochemistry.* 47:2190–2198.

9. Kiessling, V., J. M. Crane, and L. K. Tamm. 2006. Transbilayer effects of raft-like lipid domains in asymmetric planar bilayers measured by single molecule tracking. *Biophys. J.* 91:3313–3326.
10. Collins, M. D., and S. L. Keller. 2008. Tuning lipid mixtures to induce or suppress domain formation across leaflets of unsupported asymmetric bilayers. *Proc. Natl. Acad. Sci. USA.* 105:124–128.
11. Hamada, T., Y. Miura, …, M. Takagi. 2008. Construction of asymmetric cell-sized lipid vesicles from lipid-coated water-in-oil microdroplets. *J. Phys. Chem. B.* 112:14678–14681.
12. Collins, M. D. 2008. Interleaflet coupling mechanisms in bilayers of lipids and cholesterol. *Biophys. J.* 94:L32–L34.
13. May, S. 2009. Trans-monolayer coupling of fluid domains in lipid bilayers. *Soft Matter.* 5:3148–3156.
14. Schmidt, C. F., Y. Barenholz, …, T. E. Thompson. 1978. Monolayer coupling in sphingomyelin bilayer systems. *Nature.* 271:775–777.
15. Schram, V., and T. E. Thompson. 1995. Interdigitation does not affect translational diffusion of lipids in liquid crystalline bilayers. *Biophys. J.* 69:2517–2520.
16. Merkel, R., E. Sackmann, and E. Evans. 1989. Molecular friction and epitactic coupling between monolayers in supported bilayers. *J. Phys.* (*Paris*). 50:1535–1555.
17. Filippov, A., G. Orädd, and G. Lindblom. 2006. Sphingomyelin structure influences the lateral diffusion and raft formation in lipid bilayers. *Biophys. J.* 90:2086–2092.
18. Chiantia, S., P. Schwille, …, E. London. 2011. Asymmetric GUVs prepared by MβCD-mediated lipid exchange: an FCS study. *Biophys. J.* 100:L1–L3.
19. Heinemann, F., V. Betaneli, …, P. Schwille. 2012. Quantifying lipid diffusion by fluorescence correlation spectroscopy: a critical treatise. *Langmuir.* 28:13395–13404.
20. Stöckl, M. T., and A. Herrmann. 2010. Detection of lipid domains in model and cell membranes by fluorescence lifetime imaging microscopy. *Biochim. Biophys. Acta.* 1798:1444–1456.
21. Stöckl, M., A. P. Plazzo, …, A. Herrmann. 2008. Detection of lipid domains in model and cell membranes by fluorescence lifetime imaging microscopy of fluorescent lipid analogues. *J. Biol. Chem.* 283:30828–30837.
22. McIntyre, J. C., and R. G. Sleight. 1991. Fluorescence assay for phospholipid membrane asymmetry. *Biochemistry.* 30:11819–11827.
23. Cheng, H. T., and E. London. 2011. Preparation and properties of asymmetric large unilamellar vesicles: interleaflet coupling in asymmetric vesicles is dependent on temperature but not curvature. *Biophys. J.* 100:2671–2678.
24. Cheng, H. T., Megha, and E. London. 2009. Preparation and properties of asymmetric vesicles that mimic cell membranes: effect upon lipid raft formation and transmembrane helix orientation. *J. Biol. Chem.* 284:6079–6092.
25. Kucherak, O. A., S. Oncul, …, A. S. Klymchenko. 2010. Switchable Nile red-based probe for cholesterol and lipid order at the outer leaflet of biomembranes. *J. Am. Chem. Soc.* 132:4907–4916.
26. Straume, M., and B. J. Litman. 1987. Equilibrium and dynamic structure of large, unilamellar, unsaturated acyl chain phosphatidylcholine vesicles. Higher order analysis of 1,6-diphenyl-1,3,5-hexatriene and 1-[4-(trimethylammonio)phenyl]- 6-phenyl-1,3,5-hexatriene anisotropy decay. *Biochemistry.* 26:5113–5120.
27. Chiantia, S., A. S. Klymchenko, and E. London. 2012. A novel leaflet-selective fluorescence labeling technique reveals differences between inner and outer leaflets at high bilayer curvature. *Biochim. Biophys. Acta.* 1818:1284–1290.
28. Iwabuchi, K., H. Nakayama, …, K. Takamori. 2010. Significance of glycosphingolipid fatty acid chain length on membrane microdomain-mediated signal transduction. *FEBS Lett.* 584:1642–1652.
29. Sonnino, S., A. Prinetti, …, K. Iwabuchi. 2009. Role of very long fatty acid-containing glycosphingolipids in membrane organization and cell signaling: the model of lactosylceramide in neutrophils. *Glycoconj. J.* 26:615–621.
30. Quinn, P. J. 2010. A lipid matrix model of membrane raft structure. *Prog. Lipid Res.* 49:390–406.
31. Koynova, R., and M. Caffrey. 1998. Phases and phase transitions of the phosphatidylcholines. *Biochim. Biophys. Acta.* 1376:91–145.
32. Tada, K., K. Saito, …, S. Kaneshina. 2008. High-pressure study on bilayer phase behavior of oleoylmyristoyl- and myristoyloleoyl-phosphatidylcholines. *Biophys. Chem.* 138:36–41.
33. Mihailescu, M., R. G. Vaswani, …, S. H. White. 2011. Acyl-chain methyl distributions of liquid-ordered and -disordered membranes. *Biophys. J.* 100:1455–1462.
34. Kucerka, N., S. Tristram-Nagle, and J. F. Nagle. 2005. Structure of fully hydrated fluid phase lipid bilayers with monounsaturated chains. *J. Membr. Biol.* 208:193–202.
35. Chiu, S. W., E. Jakobsson, …, H. L. Scott. 1999. Combined Monte Carlo and molecular dynamics simulation of fully hydrated dioleyl and palmitoyl-oleyl phosphatidylcholine lipid bilayers. *Biophys. J.* 77:2462–2469.
36. Hui, S. W., J. T. Mason, and C. Huang. 1984. Acyl chain interdigitation in saturated mixed-chain phosphatidylcholine bilayer dispersions. *Biochemistry.* 23:5570–5577.
37. Lentz, B. R. 1993. Use of fluorescent probes to monitor molecular order and motions within liposome bilayers. *Chem. Phys. Lipids.* 64:99–116.
38. Feigenson, G. W. 2007. Phase boundaries and biological membranes. *Annu. Rev. Biophys. Biomol. Struct.* 36:63–77.
39. Nicolau, Jr., D. V., K. Burrage, …, J. F. Hancock. 2006. Identifying optimal lipid raft characteristics required to promote nanoscale protein-protein interactions on the plasma membrane. *Mol. Cell. Biol.* 26:313–323.